# Flexural performance of NSC and SCC Beam Column Joint with Headed Bar subjected to Cyclic loading

# Nambiyanna.B<sup>1</sup>, Santhosh D<sup>2</sup>, Harish M L<sup>3</sup>

<sup>1, 2, 3</sup> Assistant Professor, Department of Civil Engineering, Ramaiah Institute of Technology, Bangalore, Karnataka, India

Abstract:- Designing beam-column joints with enhanced flexural performance is crucial for constructing earthquake-resistant buildings. Ductile detailing methods are recommended for strengthening these joints, but they often lead to reinforcement congestion that NSC cannot accommodate. Self-Consolidating Concrete (SCC) with added fibres offers a solution by improving joint performance while reducing reinforcement congestion. This study investigates beam-column joints reinforced with headed bars and subjected to cyclic loading. It explores the feasibility of using SCC and NSC in combination to optimize joint design. Experimental specimens undergo reverse cyclic loading to evaluate hysteresis behaviour, stiffness degradation, ductility displacement, and failure envelopes. Results highlight the benefits of SCC with fibres and headed bars in enhancing joint resilience under seismic conditions. The findings contribute to understanding the effectiveness of these reinforcement strategies in mitigating damage and improving structural performance in earthquake-prone regions.

*Keywords:* Beam-column joints, Flexural performance, Headed bars, Self-Consolidating Concrete (SCC), NSC, Cyclic loading.

#### 1. Introduction

Earthquakes are great threat to the society. Performance of reinforced concrete structures during earthquake is very low because of absence of ductile nature consideration in reinforcement i.e. weak reinforced bond between column and beam. So, failure may occur in beam, column as well as in joint. Joints also considered as significant structural component. Exterior joints are more vulnerable to failure than do than interior ones. Seismic activity of the external beam column joint is experimentally analysed using high-strength reinforcing bars and concrete. There is increase in the energy dissipation and pinching width ratio, while not greater change in secant stiffness and average peak load (Alavi-Dehkordi, Mostofinejad, & Alaee, 2019). High performance of concrete with steel and polyolefin straight fibres are used. Behaviour of beam column joint is better in case of hybrid steel fibre combination than normal reinforced concrete and single steel fibre reinforced concrete (Annadurai & Ravichandran, 2018). HPFRCC (High performance fibre reinforced cementitious composites) material is used in joint area with various transverse reinforcement patterns to minimize the transverse reinforcement in the joint zone of exterior beam column joint. Due to the usage of HPFRCC in joints improved the load bearing ability, the energy absorption capacity and the rigidity of the members and mainly decreased the quantity of transverse reinforcements in joint zone (Nouri, Saghafi, & Golafshar, 2019). Instead of normal transverse reinforcement, continuous spiral reinforcement with SCC is implemented. Variation of the angle of reinforcement made to know the optimum angle. The experimental results show better cyclic performance with a minimum level of damage. The 80° spiral angle stirrups have better performance in load carrying capacity, energy dissipation capacity and ductility factor (Saha & Meesaraganda, 2019). Vidjeapriya et al. (Vidjeapriya & Jaya, 2013) studied a precast concrete specimens connected by a cleat angle with stiffeners. This reduced the load carrying capacity but shown acceptable behaviour in terms of energy dissipation and ductility. Through using double stiffeners, the performance of the specimens was improved. H Yang et al. (Yang, Zhao, Zhu, & Fu, 2018) had performed the experimental investigation on the different loading criteria in the beam-column joints and compared their cyclic performance for the different loading patterns. It showed that beam end loading condition is suitable for the

laboratory performance than the column end loading. Salim et al. (Barbhuiya & Choudhury, 2015) analysed the effect of beam column joint sizes. The size variation increased the brittleness, with a lot of Energy dissipation and stress changes that took place. The impact of glass fibres on normal concrete and self-compacting concrete SCC are analysed. Workability of SCC slightly reduced due to added glass fibres but Compressive and Split tensile strength are higher than normal concrete(Ahmad, Umar, & Masood, 2017). Application of basalt fibres with a varying percentage and high-grade concrete in reinforced concrete. As a result, fibres reduces the size of the crack pattern during failure and the fibre reinforced beam-column joint shows better strength and toughness performance(Sudha & Mohan, 2019). Polyethylene terephthalate (PET) fibre were used in beam column connection. This showed minimum damage and improved the seismic performance. It showed PET fibres are suitable substitute for the steel fibres as a discrete reinforcement in structures (Marthong & Marthong, 2016). Abbas et al. (Abbas, Ali, & Waryoosh, 2018) studied behaviour of reinforced concrete frames. Monolithically casting with steel fibre variation was done in the experiments. Usage of steel fibres effetely decreased the beam deflection and increased load carrying capacity and stiffness. Fahmy et al. (Fahmy, Farghal, & Sharobeem, 2018) done experimental study for the seismic behavior on external beam column joints with differentiation of longitudinal reinforcement for columns. They stated that splicing in column reinforcement reduced deformability of joint. Adding BFRP (basalt fibre reinforced polymer) rebars to BCJ acts as damage controllable bars that reduces both serviceability damage and joint shear deformation to failure. The effect of hybrid fibres on the beam column joint was tested experimentally with the variance of crimped steel fibres and polypropylene fibres. Its beam column joint strength and its ductility are improved by the use of hybrid fibres(Ganesan, Indira, & Sabeena, 2014). Bilal H et al. (Hamad & Ibrahim, 2009) explained the effect of hooked bars in the beam-column joint region. The test results showed that bond performance ultimately increased on introducing hooked bars. Increase on the percentage of fibres showed a gradual increase in ultimate load. Header bars and self-consolidating concrete used in exterior beam-column joints. Specimens was observed to enhance the joint seismic behaviour and nearly similar behaviour observed in both relative head area(Paknejadi & Behfarnia, 2020). Ashish et al. (Ugale & Khante, 2020) done the experimental investigation to know the role of Headed bar and different types of lateral reinforcement in beam column joint. Results shows that there is enhancement in the behaviour of the structure mainly in the energy dissipation capacity.

It is observed from the literature review that various research works on beam column joint carried out using different reinforcement patterns, materials for construction and percentage of fibres. Limited work has been done for variation of steel fibres and headed bar usage in the plastic hinge region. Therefore, for the current study, experimental work on the exterior beam column joint with Normal and Self compacting concrete and results are evaluated by comparing the control specimen that does not contain steel fibres.

#### 2. Experimental Program

#### 2.1 Materials and Mix proportion

Ordinary Portland Cement of 53 grade, manufactured sand as fine aggregates, coarse aggregate of 12.5 mm down size, Fly ash, AURAMIX 400 superplasticizer, Viscosity modifying agent, Flat Crimped Steel fibres and Fe500 deformed steel bar are used in construction of concrete specimens. The mix proportion is developed according to the guidelines Specification IS 10262-2009. Table 2.1 indicates the descriptions mix proportion of NSC and SCC, which are used for casting. Results of a test conducted on the Hardened propertied of NSC and fresh properties of SCC has been shown in Table 2.2 and 2.3 respectively.

**Table** *Error! No text of specified style in document.***1: Mix proportion** 

Materials		Mix	
	NSC	SCC	
Cement (kg/m3)	380	214.28	
Fly ash (kg/m3)	0	341.1	
Fine aggregates (kg/m3)	802.32	821.59	
Coarse aggregates (kg/m3)	936.6	692.5	

Water (kg/m3)	202.5	155.508
Super- plasticizer (kg/m3)	0	6.03
VMA (kg/m3)	0	0.821

Table Error! No text of specified style in document..2: Hardened properties of NSC

% fibre	Compressive strength	Flexural strength	
	Mpa	Mpa	
0	32.5	4.09	
0.75	41	5.85	

Table Error! No text of specified style in document..3: Fresh properties of SCC

% fibre	Slump value	L-box	U-box	V-funnel time
	mm	S	S	s
0	700	4	3	4
0.75	620	6.9	6.8	9

# 2.2 Details of Test Specimens

Table Error! No text of specified style in document..4: Beam column joint specimens' details

S No	Specimens type (IS 13920-2016)	Description	Beam reinforcement	Column reinforcement	Transverse reinforcement at
					50 mm spacing
1	BCJ 31	NSC/0%	4 #10 Ø	4 #12 Ø	2L- 8 Ø
2	BCJ 32	NSC/0.75%	4 #10 Ø	4 #12 Ø	2L- 8 Ø
3	BCJ 33	NSC/H/0%	4 #10 Ø	4 #12 Ø	2L- 8 Ø
4	BCJ 34	NSC/H/0.75%	4 #10 Ø	4 #12 Ø	2L- 8 Ø
5	BCJ 35	SCC/0%	4 #10 Ø	4 #12 Ø	2L- 8 Ø
6	BCJ 36	SCC/0.75%	4 #10 Ø	4 #12 Ø	2L- 8 Ø
7	BCJ 37	SCC/H/0%	4 #10 Ø	4 #12 Ø	2L- 8 Ø
8	BCJ 38	SCC/H/0.75%	4 #10 Ø	4 #12 Ø	2L- 8 Ø



Figure Error! No text of specified style in document..1. Headed bar reinforcement details

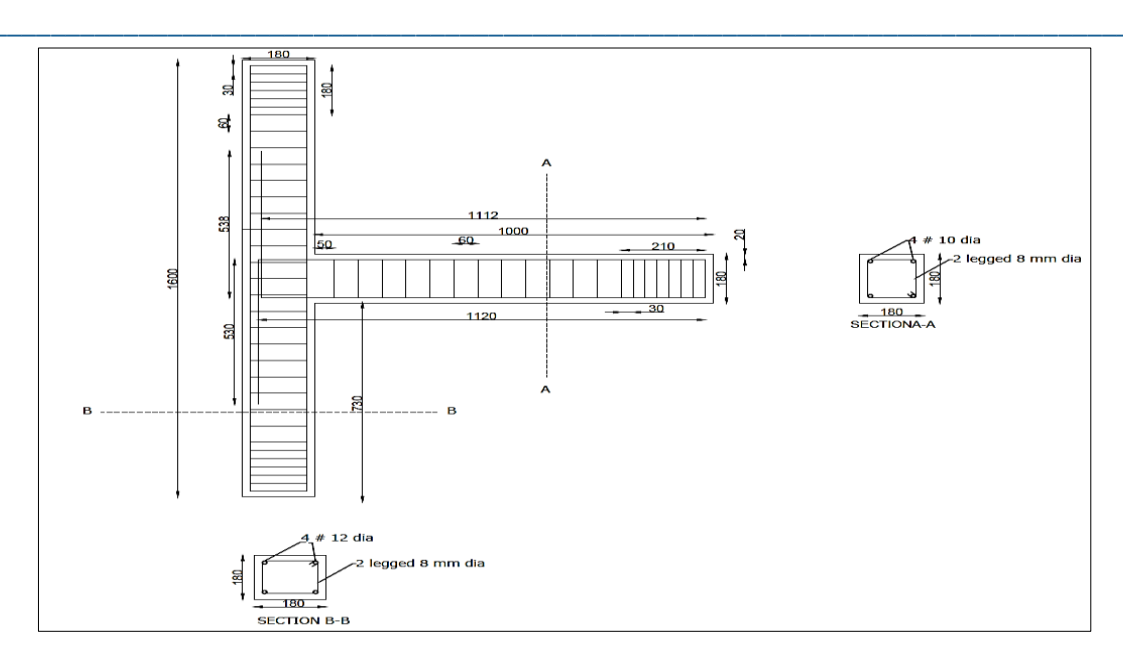


Figure Error! No text of specified style in document..2. Typical Reinforcement details for BCJ specimens

# 2.3 Preparation of formwork

Formwork is made up of plywood sheets as shown in figure 2.3. The carpentry work is done so that the required size is achieved, the inside surface of plywood is oiled before casting in order to make demolding easier. 20mm cover blocks are used at the bottom of the formwork above which reinforcement cage is placed as shown in figure 2.4.

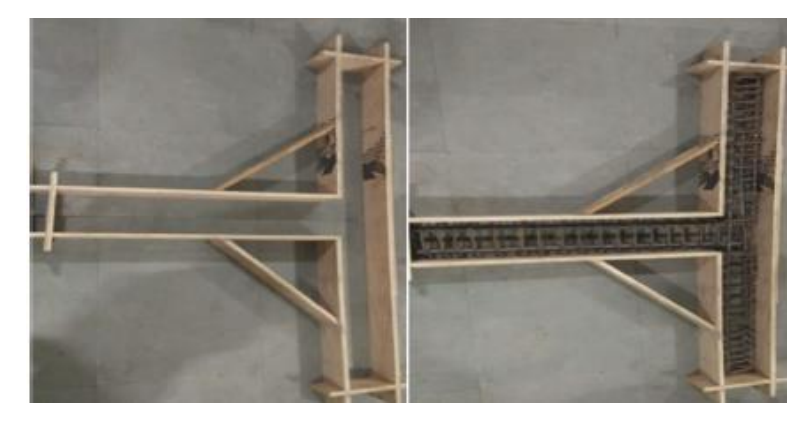


Figure Error! No text of specified style in document..3. Preparation of Formwork and Placing of Reinforcement Cage



Figure Error! No text of specified style in document. 4. Formwork with Reinforcement Cage

#### 2.4 Mixing of concrete and Casting of specimens

First four specimens were made with NSC type concrete and constituents were cement, fine aggregate, coarse aggregate, water and steel fibres. Other four specimens with SCC type concrete and constituents were cement, fine aggregate, coarse aggregate, water, GGBS, Fly ash and steel fibres. All these constituents are weighed. Pan mixer was used to achieve a homogeneous mixture. The required amount of steel fibres was added during mixture for SFRNSC and SFRSCC specimen then mixed concrete was poured to formwork. The vibrator was used for the proper compaction and also to avoid honeycombing. The top surface of the beam and column was leveled. Final finished view of the specimen is as shown in 2.5.



Figure Error! No text of specified style in document..5. Casting of specimens

#### 2.5 Curing

Curing is performed after 24hours by putting gunny bags on retrofitted area and watering it for 28days. After curing period, all specimens are finished by grinding the undulated edges. Specimens are whitewashed in order to visualize clear crack pattern.

# 2.6 Test Setup and Instrumentation

The test set up for all specimens along with support and some main components are shown in the figure 2.7 and Schematic Diagram of Test Setup is shown in figure 2.6. Specimens were tested in a loading frame which has 1000kN capacity. The testing was conducted in such a way that column placed vertically and the beam is parallel to ground. The column's top and bottom supports are hinged to restrict movement of column and allow only rotation. To represent the gravity load, Constant 200kN axial compression load applied on upper end of the column using a hydraulic jack. This load was applied before the test and kept constant throughout the test. All the specimens were tested under reverse cyclic loading with an increment of 10mm for every two cycles of same amplitude under displacement control. Cyclic load was applied with help of two hydraulic jacks to which load cells are connected to measure the applied loads. To measure controlled displacements, LVDT was connected at beam end. Each and every reading of LVDT and load cells were recorded using a data acquisition system.

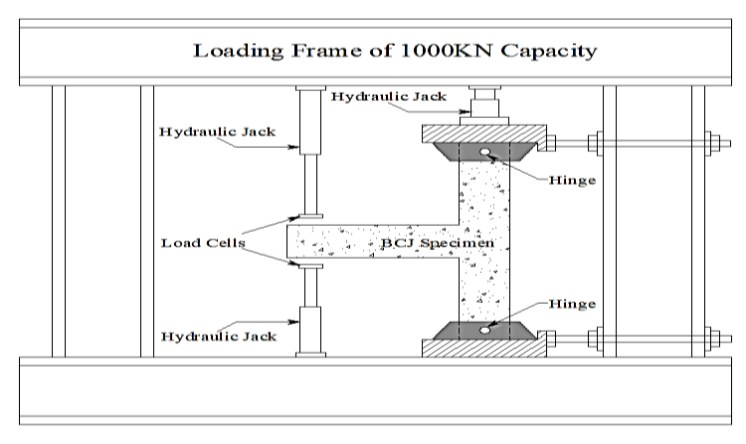


Figure Error! No text of specified style in document..6. Schematic Diagram of Test Setup

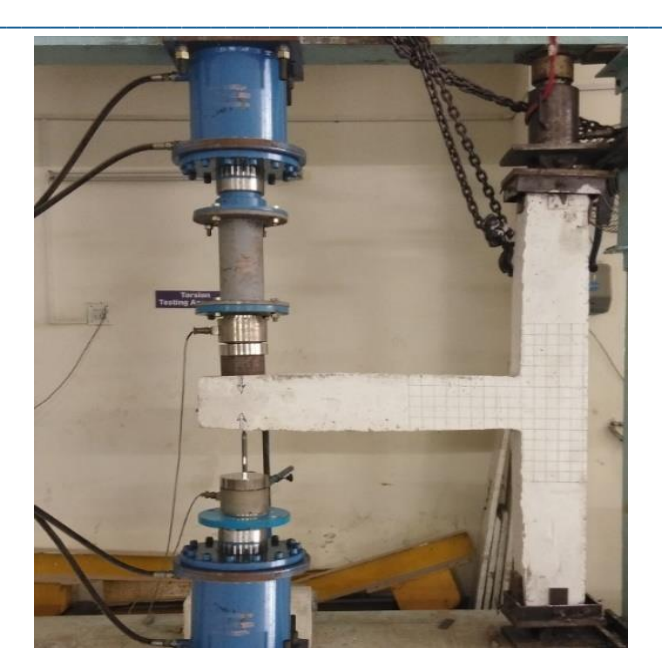


Figure Error! No text of specified style in document.. 7. Test Setup and Instrumentation

# 2.7 Cyclic Loading Protocol

Cyclic lading is carried out using two hydraulic jacks at the end of the beam. In that one is for downward load and another is used for reverse loading as in figure 2.7. The displacement history applied to all specimens is shown in figure 2.8. Total cyclic load was applied in five sets. Each set is composed of two cycles of the same displacement. And the next set was 10 mm larger than the previous one. A total of 10 cycles applied. Each cycle was split into two stages. Upper jack was loaded down at the free end of the beam during the first stage until the required vertical displacement was reached and then released. In the second stage, the beam end loaded up using the lower jack which was manually controlled until the required displacement was reached and then released. Experiment is started with displacement of 10 mm amplitude and performed up to 50 mm.

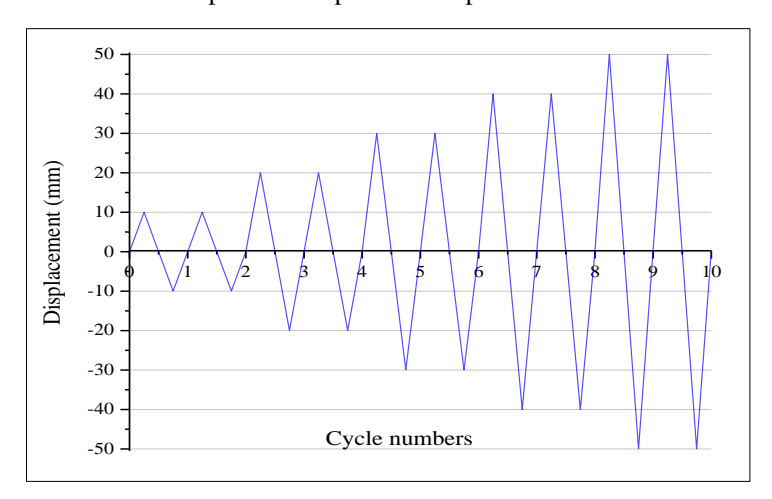


Figure Error! No text of specified style in document. 8. Cyclic Loading Protocol

#### 3. Results and Discussion

Hysteresis behaviour is the principal component in the reverse cyclic loading of BCJ, which simulates the practical situation of BCJ undergoing deformation in both the directions. It is influenced over several parameters such as grade of concrete, percentage of steel reinforcement, joint detailing, geometry of beam and column, presence of fibre, axial load ratio etc.

\_\_\_\_\_

### 3.1 NSC Specimens

# 3.1.1 Load carrying capacity and Hysteresis behaviour

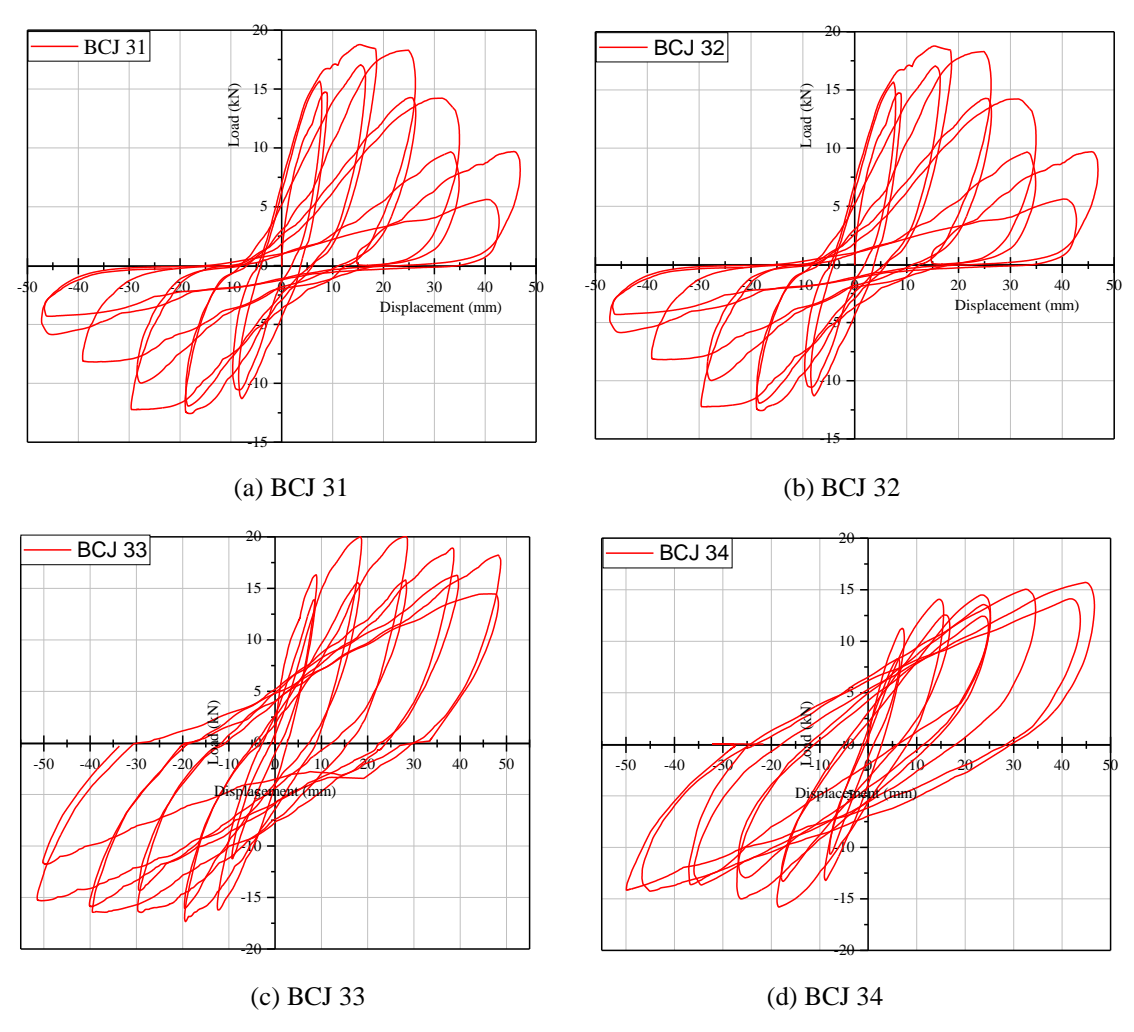


Figure Error! No text of specified style in document..9. Hysteresis curves of NSC specimens (a)BCJ 31 (b)BCJ 32 (c)BCJ 33 (d)BCJ 34

The hysteresis response of NSC specimens is depicted in Figure 3.1. Data were imported from the acquisition system, analysed in Excel, and smoothed and graphed using Origin software. The control specimen, BCJ 31, had maximum loads of 16.4 kN (positive cycle, third cycle) and 18.4 kN (negative cycle, fifth cycle). Hairline cracks propagated through the beam-column junction, causing gradual stiffness reduction. Specimen BCJ 32 showed a 6.53% increase in load-carrying capacity compared to BCJ 31, with maximum loads of 19.6 kN (positive cycle, third cycle) and 15.8 kN (negative cycle, fourth cycle). Fibre addition decreased crack width but increased micro cracks. Headed bar specimens showed no pinching effect, indicating no bond slip and less seismic demand. Specimen BCJ 33 had maximum loads of 20.4 kN (positive cycle, third cycle) and 18.3 kN (negative cycle, third cycle), a 10.87% increase over BCJ 31. Specimen BCJ 34 had maximum loads of 17.3 kN (positive cycle, third cycle) and 17.1 kN (negative cycle, fifth cycle), a 5.98% decrease compared to BCJ 31.

### 3.1.2 Stiffness Degradation

Stiffness is a measurement of resistance to deformation, is defined as the load required to cause unit deflection. Its graphical representation is as shown in figure *XX*. The maximum loads and deflection at every half-cycle (i.e. positive and negative cycle) are noted to calculate the peak stiffness of that cycle; it is found out by

 $K_i = \frac{|+P_i|+|-P_i|}{|+\delta_i|+|-\delta_i|}$  Equation *Error! No text of specified style in document.*.1: Peak to Peak stiffness

where,  $+P_i$  and  $-P_i$  are the Maximum load under  $i^{th}$  cycle of Positive and Negative cycles; and  $+\delta_i$  and  $-\delta_i$  are ultimate deflection of corresponding  $i^{th}$  cycle.

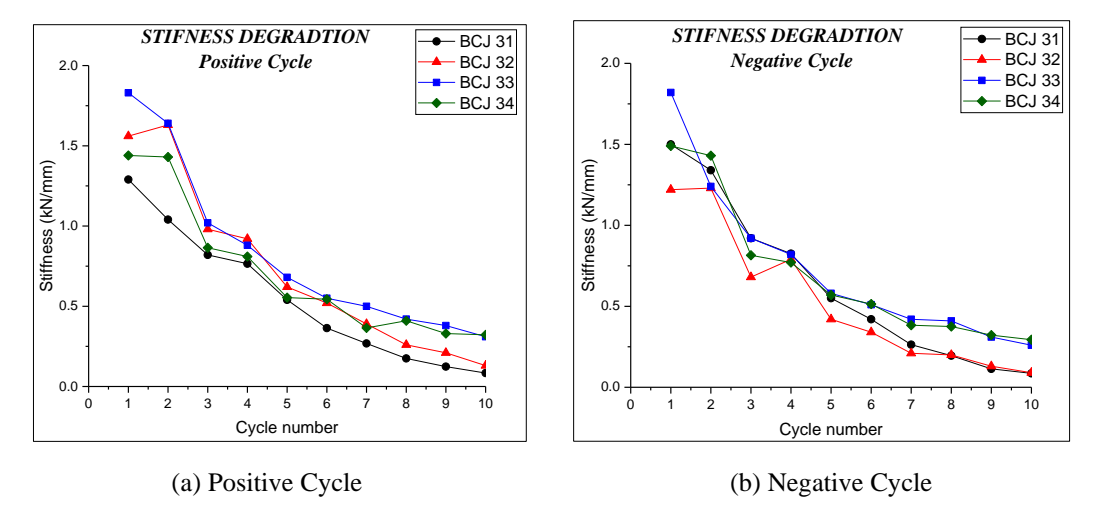


Figure Error! No text of specified style in document..10. Stiffness Degradation of NSC specimens (a) Positive cycle (b) Negative cycle

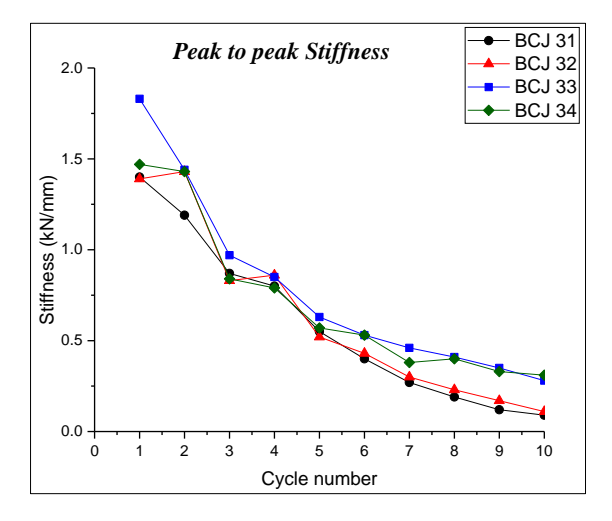


Figure Error! No text of specified style in document..11. Peak to Peak Stiffness of NSC specimens

Peak stiffness for specimens is determined using above equation for each cycle and is shown in figure 3.3. It is evident that the performance of Headed bar in BCJ exhibits a noteworthy agreement in terms of stiffness degradation. Specifically, specimen BCJ 33 demonstrates an improvement in peak-to-peak stiffness during the last load cycle compared to the other specimens.

# 3.1.3 Displacement Ductility

One of the essential characteristics of structural element is Ductility. This is explained as structural element's ability to withstand greater deformations above yield, without losing too much of its capacity to carry load. Brittle failure does not show any warning before failure, so it must be avoided. Ductile behaviour of structure gives greater deformation nearer ultimate loads. Plastic deformation of the member is proportional to its amount of Ductility. In general, ductility was calculated using a ratio called the ductility factor. This is normally measured as the ratio of deflection at the ultimate load and at yield load i.e. displacement ductility factor =  $\frac{\delta u}{\delta v}$ 

where  $\delta u$  = Ultimate or Maximum deflection and  $\delta v$  = Yield deflection.

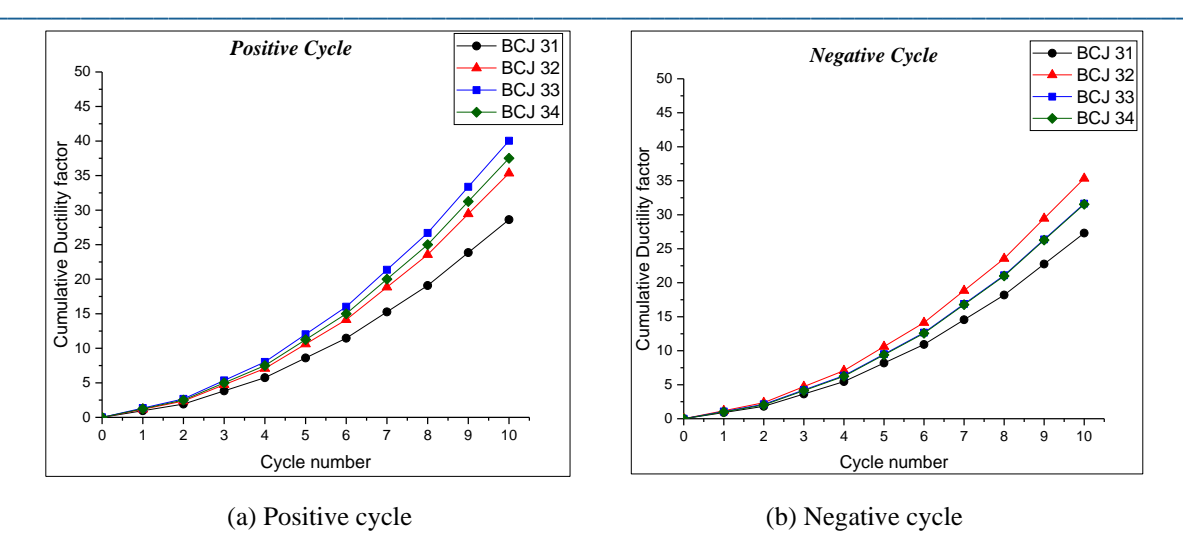


Figure Error! No text of specified style in document..12. Cumulative ductility factor for NSC specimens
(a)Positive cycle (b)Negative cycle

Yield deflection is obtained by the horizontal distance between the origin and point of intersection of the tangent drawn to a curve of the first cycle and curve of the maximum load for both positive and negative cycle. The cumulative ductility factor is defined as the amount of the ductility at the maximum load level obtained in each cycle up to the cycles considered. Figure 3.4 represents Cumulative ductility factor for NSC specimens. Significant improvement in the ductility behaviour was observed over the specific technique of headed bars in BCJ.

#### 3.1.4 Energy Dissipation

Structural ductile behaviour can also be described by Energy dissipation. It is determined from area enclosed under each hysteric loop (i.e. area of load displacement curve). The energy of individual cycles is computed using Origin lab software and cumulative energy dissipated for 10 cycles is tabulated which shown in figure 3.5 and 3.6. Higher energy dissipation for rest specimens than control specimen because of higher load carrying capacity, and reduction of pinching and expansion of hysteresis loops.

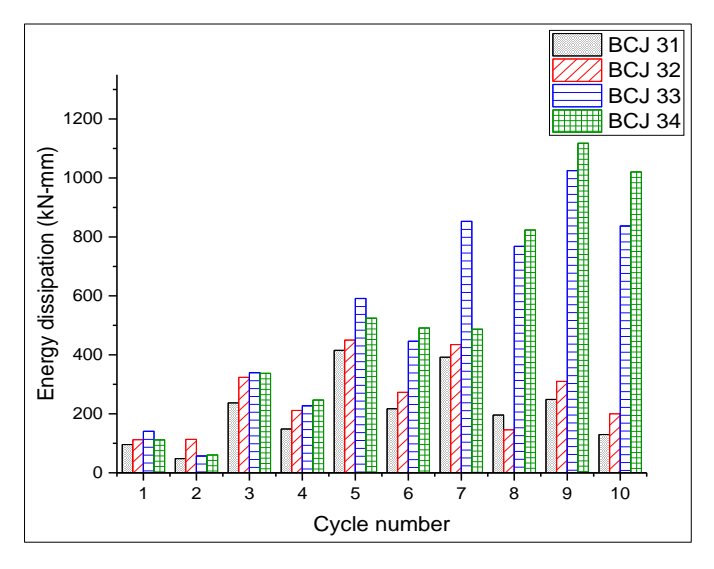


Figure Error! No text of specified style in document..13. Energy dissipation of NSC specimens

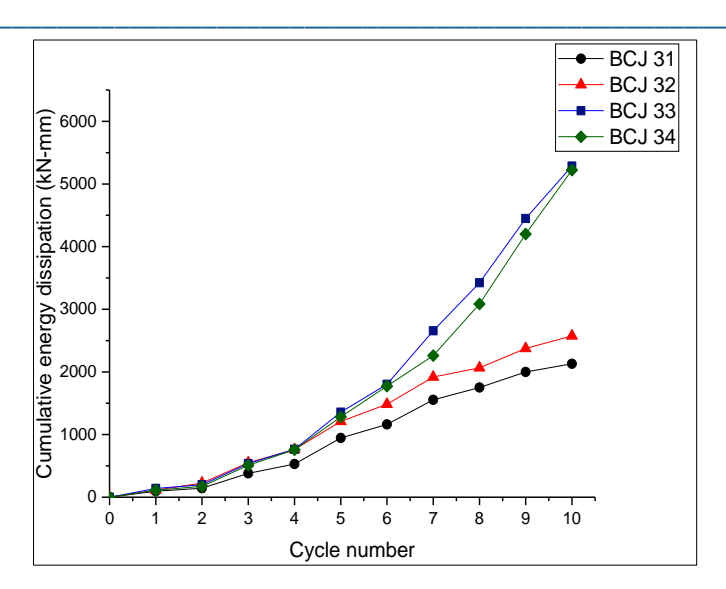
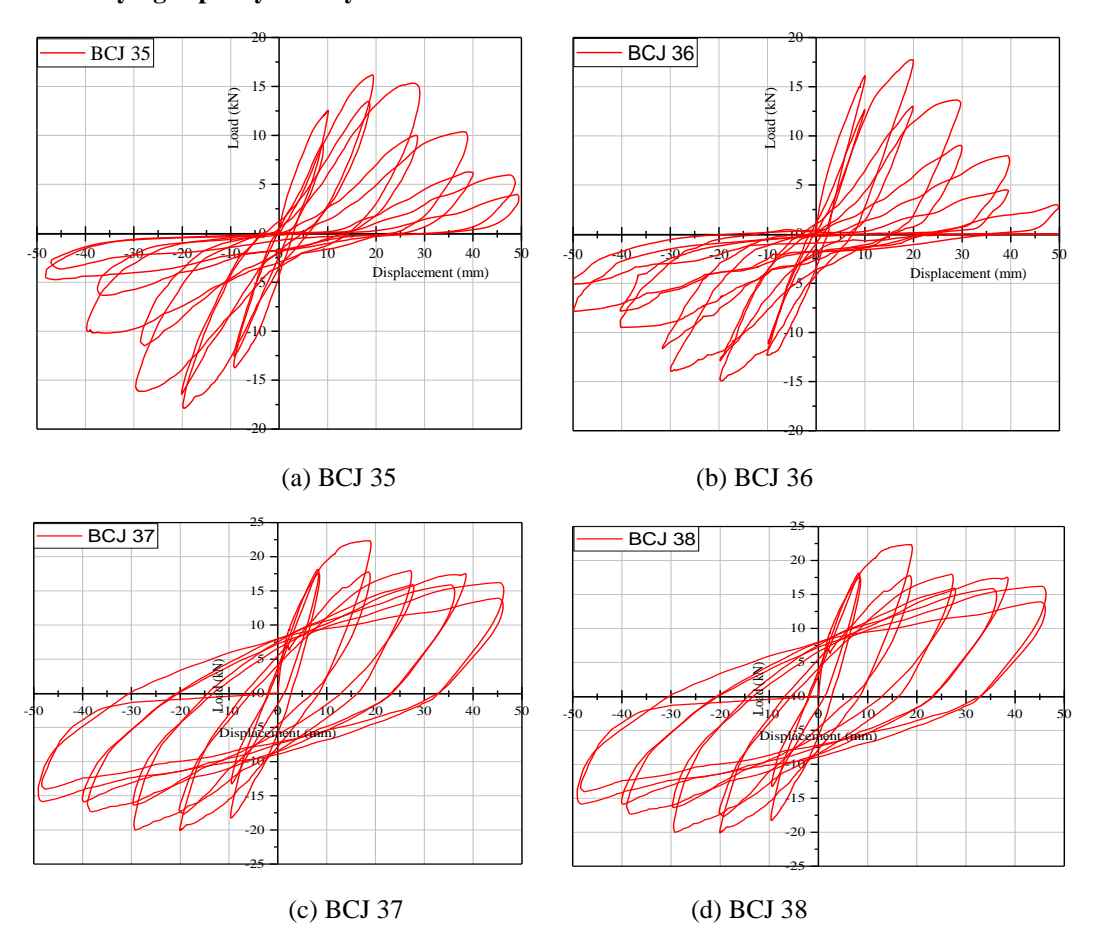


Figure Error! No text of specified style in document..14. Cumulative energy dissipation of NSC specimens

The observation made from **Error! Reference source not found.** 3.5, regarding energy absorption of the joint indicated participation of the Headed bar while enhancing the energy absorption. Increase in the energy of the specimens with Heded bars were found to be about 1.65 times higher compared over control specimen without headed bars.

# 3.2 SCC Specimens

# 3.2.1 Load carrying capacity and Hysteresis behaviour



# Figure Error! No text of specified style in document..15. Hysteresis curves of SCC specimens (a)BCJ 35 (b)BCJ 36 (c)BCJ 37 (d)BCJ 38

The hysteresis response of SCC specimens is presented in Figure 3.7. The control specimen, BCJ 35, achieved maximum loads of 19.8 kN (positive cycle) and 16.4 kN (negative cycle) in the third cycle. Specimen BCJ 36 showed a 7.58% decrease in load-carrying capacity compared to BCJ 35, with maximum loads of 18.3 kN (positive cycle) and 15.2 kN (negative cycle) in the third cycle. Headed bar specimens exhibited no pinching effect, indicating no bond slip and reduced seismic demand. Specimen BCJ 37 reached maximum loads of 19.7 kN (positive cycle) and 20.6 kN (negative cycle) in the third and first cycles, respectively, showing a 4.05% increase compared to BCJ 35. Specimen BCJ 38 achieved maximum loads of 22.5 kN (positive cycle) and 20.6 kN (negative cycle) in the third cycle, but showed a 13.64% decrease compared to BCJ 35.

### 3.2.2 Stiffness Degradation

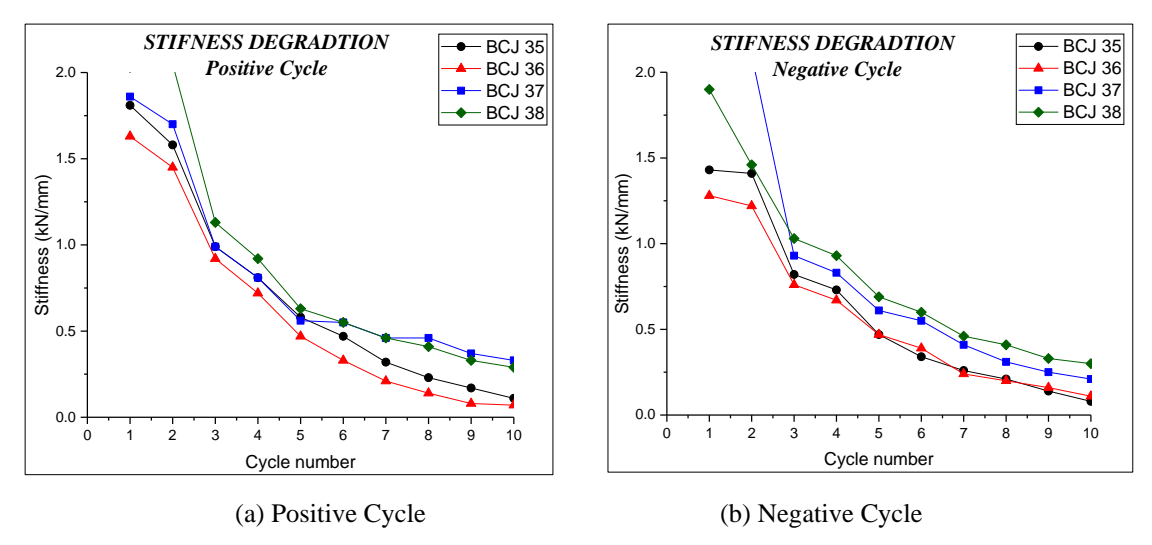


Figure Error! No text of specified style in document..16. Stiffness Degradation of SCC specimens (a) Positive cycle (b) Negative cycle

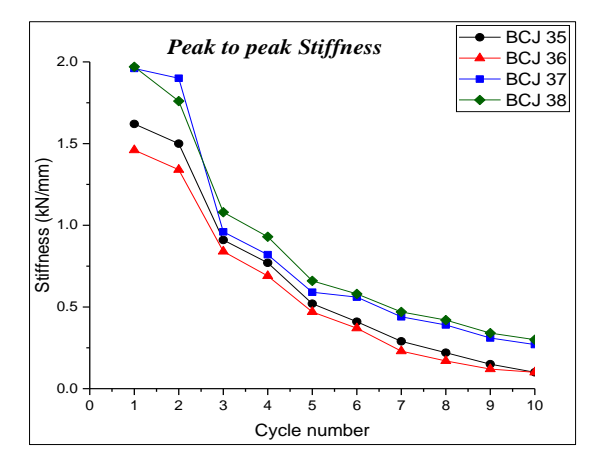


Figure Error! No text of specified style in document..17. Peak to Peak Stiffness of SCC specimens

Stiffness is a measurement of resistance to deformation and is represented graphically as shown in figure 3.8. Peak stiffness for specimens is calculated by equation 3.1 and shown in figure 3.9. The performance of the Headed bar in BCJ shows a significant correlation with stiffness degradation. Notably, specimen BCJ 38 exhibits an enhancement in peak-to-peak stiffness during the final load cycle compared to the other specimens.

#### 3.2.3 Displacement Ductility

Ductility is structural element's ability to withstand greater deformations above yield, without losing too much of its capacity to carry load. Displacement Ductility factor is measured as the ratio of deflection at the maximum load and at yield load.

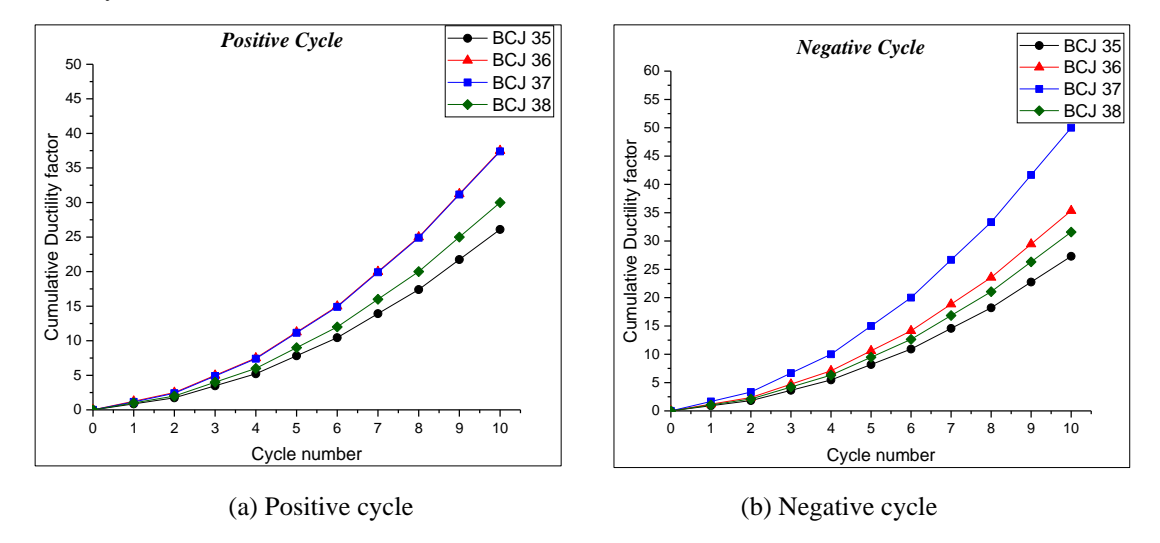


Figure Error! No text of specified style in document..18. Cumulative ductility factor for SCC specimens
(a)Positive cycle (b)Negative cycle

The cumulative ductility factor is defined as the amount of the ductility at the maximum load level obtained in each cycle up to the cycles considered. Figure 3.10 depicts the cumulative ductility factor for SCC specimens. A notable improvement in ductility behaviour was observed with the use of headed bars in specimen BCJ 37.

#### 3.2.4 Energy Dissipation

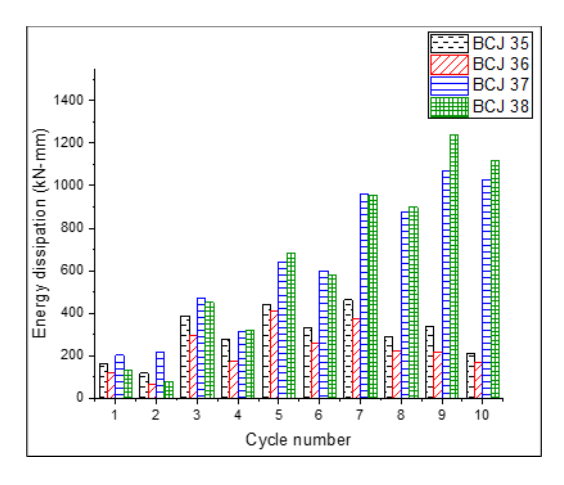


Figure Error! No text of specified style in document..19. Energy dissipation of SCC specimen

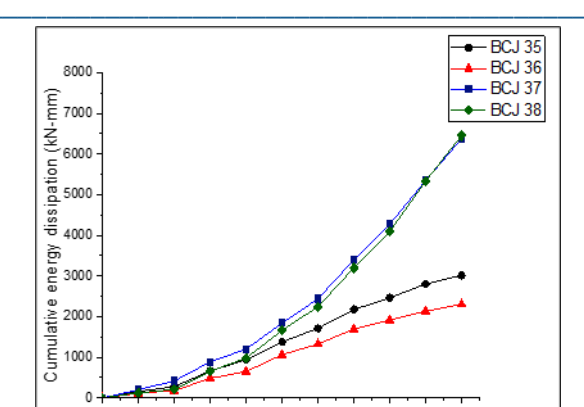


Figure Error! No text of specified style in document. 20. Cumulative energy dissipation of SCC specimens

Observations from Figure 3.12 indicate that the use of Headed bars enhances the energy absorption of the joint. The energy absorption of specimens with Headed bars was approximately 1.2 times higher than that of the control specimen without Headed bars.

#### 4. Conclusions

This study investigates the flexural behavior and seismic performance of beam-column joints, specifically comparing specimens with headed bars, NSC, and Self-Consolidating Concrete (SCC). The research examines critical parameters such as, load-carrying capacity, stiffness, ductility factors, and energy dissipation. The findings offer insights into the comparative advantages and performance enhancements provided by different reinforcement techniques and concrete types under cyclic loading conditions.

The flexural behavior of headed bar specimens was superior to that of conventional reinforced specimens, exhibiting smaller crack widths, better crack patterns, and enhanced ductility. Initial cracks were observed within the first 10mm of deflection, and the addition of fibres reduced crack width but increased the number of micro cracks. Hysteresis curves indicated a pinching effect in all specimens except those with headed bars, suggesting the presence of bond slip mechanisms.

For NSC specimens, the load-carrying capacity increased for BCJ 32 and BCJ 33, while it decreased for BCJ 34 compared to the control specimen BCJ 31. Additionally, peak-to-peak stiffness values for BCJ 32, BCJ 33, and BCJ 34 showed improvements. Cumulative ductility factors and energy dissipation also increased for these specimens in both positive and negative cycles compared to BCJ 31.

In SCC specimens, BCJ 36's load-carrying capacity decreased, whereas it increased for BCJ 37 and BCJ 38 compared to the control specimen BCJ 35. Peak-to-peak stiffness values for BCJ 36, BCJ 37, and BCJ 38 improved as well. Moreover, cumulative ductility factors for these SCC specimens saw increases in both positive and negative cycles compared to BCJ 35, with cumulative energy dissipation also showing notable improvements for BCJ 32, BCJ 33, and BCJ 34 compared to BCJ 31.

**Acknowledgements:** We sincerely acknowledge the support of Department of Civil Engineering, Ramaiah Institute of Technology Bangalore for the support extended during this investigation.

**Author contributions:** All authors contributed to the study conception and design. Material preparation, data collection and analysis were performed by [NB], [DS] and [HM]. The first draft of the manuscript was written by [NB] and all authors commented on previous versions of the manuscript. All authors read and approved the final manuscript.

# **Declarations:**

Conflict of interest "On behalf of all authors, the corresponding author states that there is no conflict of interest".

#### References

[1] Abbas, A. N., Ali, S. K., & Waryoosh, W. A. (2018). Behavior of Reinforced Concrete Frames with Different

- [1] Abbas, A. N., Ali, S. K., & Waryoosh, W. A. (2018). Behavior of Reinforced Concrete Frames with Different Beam-column Joints Types. International Journal of Applied Engineering Research, 13(11), 9450–9456.
- [2] Ahmad, S., Umar, A., & Masood, A. (2017). Properties of Normal Concrete, Self-compacting Concrete and Glass Fibre-reinforced Self-compacting Concrete: An Experimental Study. Procedia Engineering, 173, 807–813. https://doi.org/10.1016/j.proeng.2016.12.106
- [3] Alavi-Dehkordi, S., Mostofinejad, D., & Alaee, P. (2019). Effects of high-strength reinforcing bars and concrete on seismic behavior of RC beam-column joints. Engineering Structures, 183(July 2018), 702–719. https://doi.org/10.1016/j.engstruct.2019.01.019
- [4] Annadurai, A., & Ravichandran, A. (2018). Seismic Behavior of Beam—Column Joint Using Hybrid Fibre Reinforced High-Strength Concrete. Iranian Journal of Science and Technology Transactions of Civil Engineering, 42(3), 275–286. https://doi.org/10.1007/s40996-018-0100-9
- [5] Barbhuiya, S., & Choudhury, A. M. (2015). A study on the size effect of RC beam-column connections under cyclic loading. Engineering Structures, 95, 1–7. https://doi.org/10.1016/j.engstruct.2015.03.052
- [6] Fahmy, M. F. M., Farghal, O. A., & Sharobeem, G. F. G. (2018). Exploratory study of adopting longitudinal column reinforcement details as a design-controllable tool to seismic behavior of exterior RC beam-column joints. Engineering Structures, 174(July), 95–110. https://doi.org/10.1016/j.engstruct.2018.07.050
- [7] Ganesan, N., Indira, P. V., & Sabeena, M. V. (2014). Behaviour of hybrid fibre reinforced concrete beam-column joints under reverse cyclic loads. Materials and Design, 54, 686–693. https://doi.org/10.1016/j.matdes.2013.08.076
- [8] Hamad, B. S., & Ibrahim, F. G. (2009). Effect of FRP confinement on bond strength of hooked bars: Normal-strength concrete structures. Journal of Composites for Construction, 13(4), 279–291. https://doi.org/10.1061/(ASCE)1090-0268(2009)13:4(279)
- [9] Marthong, C., & Marthong, S. (2016). An experimental study on the effect of PET fibres on the behavior of exterior RC beam-column connection subjected to reversed cyclic loading. Structures, 5, 175–185. https://doi.org/10.1016/j.istruc.2015.11.003
- [10] Nouri, A., Saghafi, M. H., & Golafshar, A. (2019). Evaluation of beam-column joints made of HPFRCC composites to reduce transverse reinforcements. Engineering Structures, 201(October). https://doi.org/10.1016/j.engstruct.2019.109826
- [11] OriginLab Corporation. (2018). OriginPro (Version 2018). OriginLab Corporation.
- [12] Paknejadi, A. H., & Behfarnia, K. (2020). Performance of reinforced self-consolidating concrete beam-column joints with headed bars subjected to pseudo-static cyclic loading. Ain Shams Engineering Journal, (xxxx). https://doi.org/10.1016/j.asej.2019.12.008
- [13] Saha, P., & Meesaraganda, L. V. P. (2019). Experimental investigation of reinforced SCC beam-column joint with rectangular spiral reinforcement under cyclic loading. Construction and Building Materials, 201, 171–185. https://doi.org/10.1016/j.conbuildmat.2018.12.192
- [14] Sudha, C., & Mohan, G. (2019). Behaviour of fibre reinforced concrete using Basalt fibre in Beam column joint under cyclic loading. ARPN Journal of Engineering and Applied Sciences, 14(8), 1463–1470.
- [15] Ugale, A. B., & Khante, S. N. (2020). Study of energy dissipation of reinforced concrete beam-column joint confined using varying types of lateral reinforcements. Materials Today: Proceedings, 27(xxxx), 1356–1361. https://doi.org/10.1016/j.matpr.2020.02.690
- [16] Vidjeapriya, R., & Jaya, K. P. (2013). Experimental study on two simple mechanical precast beam-column connections under reverse cyclic loading. Journal of Performance of Constructed Facilities, 27(4), 402–414. https://doi.org/10.1061/(ASCE)CF.1943-5509.0000324
- [17] Yang, H., Zhao, W., Zhu, Z., & Fu, J. (2018). Seismic behavior comparison of reinforced concrete interior beam-column joints based on different loading methods. Engineering Structures, 166(October 2017), 31–45. https://doi.org/10.1016/j.engstruct.2018.03.022